

Performance Comparison of Electronic PMD Equalizers for Coherent PDM QPSK Systems

Nikolaos Mantzoukis, Constantinos S. Petrou, *Member, IEEE*, Athanasios Vgenis, Ioannis Roudas, *Member, IEEE*, and Thomas Kamalakis

Abstract—Polarization division multiplexed (PDM) quadrature phase-shift keying (QPSK) coherent optical systems employ blind adaptive linear electronic equalizers for polarization-mode dispersion (PMD) compensation. In this paper, we compute the performance of various adaptive, fractionally spaced, feed-forward electronic equalizers, using the outage probability as a criterion. A parallel programming implementation of the multicanonical Monte Carlo method is developed, which automatically performs concurrent loop computation on multicore processors, for the estimation of the tails of the outage probability distribution. The constant modulus algorithm (CMA), the decision-directed least mean squares (DD-LMS), and their combination are applied for the adaptation of electronic equalizer filter coefficients. In the exclusive presence of PMD, we demonstrate that half-symbol-period-spaced CMA-based adaptive electronic equalizers perform slightly better than their DD-LMS counterparts, at links with strong PMD, whereas the opposite holds true at the weak PMD regime. It is shown that the successive application of CMA and DD-LMS with 20 complex, half-symbol-period-spaced taps per finite impulse response filter is adequate to reduce the outage probability of coherent PDM QPSK systems to less than 10^{-5} , for a mean differential group delay of more than twice the symbol period.

Index Terms—Multicanonical Monte Carlo (MMC), optical communications, outage probability, parallel programming, polarization-mode dispersion (PMD).

I. INTRODUCTION

POLARIZATION DIVISION MULTIPLEXED (PDM) quadrature phase-shift keying (QPSK) coherent optical communications systems use digital signal processing (DSP) to counteract transmission impairments. Among the most important DSP functionalities in coherent receivers are polarization demultiplexing and equalization. Adaptive, blind, multiple-input multiple-output (MIMO) linear electronic equalizers are used, in order to counteract rapid polarization

rotations, perform polarization demultiplexing, and combat polarization-mode dispersion (PMD) and polarization-dependent loss (PDL) [1]–[4]. However, due to the limited length of their finite impulse response (FIR) filters [1], as well as to singularities in their coefficient adaptation algorithms [4]–[6], these equalizers cannot fully eliminate outages, even after equalization. Therefore, there is always a nonnegligible, albeit small, outage probability, even after equalization.

The impact of PMD on the outage probability of intensity modulation/direct detection optical communication systems has been thoroughly studied [7]–[22]. In contrast, there is a limited number of similar theoretical studies for coherent optical systems [23]–[29]. Recent publications use rudimentary PMD emulators (PMDEs) consisting of one or two birefringent sections [9], [10], [28], [29] in order to demonstrate an almost unlimited first-order (and, to some extent, second-order) PMD compensation [1], [9], [10] provided that the electronic equalizers have a sufficient number of taps per FIR filter [27]. However, from a system design point of view, it is important to accurately compute the performance of coherent PDM QPSK systems in the presence of higher order PMD and to provide guidelines for the design of adaptive PMD equalizers.

This paper presents an in-depth simulation study of the performance of linear electronic PMD equalizers in coherent PDM QPSK optical communications systems. Several equalizer coefficient adaptation algorithms are compared using the outage probability as a performance criterion. The latter is very difficult to evaluate, since outages in a system employing equalization occur very rarely. Even experimental measurements may prove inadequate to assess system performance [2]–[4]. Resorting to conventional Monte Carlo (MC) simulations to estimate the probability of such rare PMD outages is impractical, as it requires a prohibitively large number of iterations. Alternatively, it is possible to use importance sampling methods [16], [17], such as the multicanonical Monte Carlo (MMC) method [30]–[37], in order to reduce the simulation time required to estimate the statistics of these rare events. Furthermore, in this paper, we use a parallel implementation of the MMC method, similar to [37], for the efficient evaluation of the outage probability of a coherent PDM QPSK system after PMD equalization.

We compare the performance of three popular adaptive, PMD electronic equalizers, namely, the constant modulus algorithm (CMA) [38], the decision-directed least mean squares (DD-LMS) algorithm [25], and their combination [4].

We show that, in the exclusive presence of PMD, both CMA- and DD-LMS-based PMD equalizers, with as few as ten $T_s/2$ -spaced taps per FIR filter (where T_s is the symbol

Manuscript received July 28, 2010; revised January 17, 2011; accepted March 22, 2011. Date of publication April 05, 2011; date of current version May 25, 2011. This paper is a part of the 03ED628 Research Project cofinanced by National and Community Funds (20% from the Greek Ministry of Development-General Secretariat of Research and Technology and 80% from E.U.-European Social Fund).

N. Mantzoukis, C. S. Petrou, A. Vgenis, and I. Roudas are with the Optical Communications Group, Department of Electrical and Computer Engineering, University of Patras, Rio 26500, Greece (e-mail: nmantzoukis@gmail.com; costas.s.petrou@gmail.com; thanvg@gmail.com; roudas@ee.upatras.gr).

T. Kamalakis is with the Department of Informatics and Telematics, Harokopio University of Athens, Athens, GR17671 Greece (e-mail: thkam@di.uoa.gr).

Color versions of one or more of the figures in this paper are available online at <http://ieeexplore.ieee.org>.

Digital Object Identifier 10.1109/JLT.2011.2136320

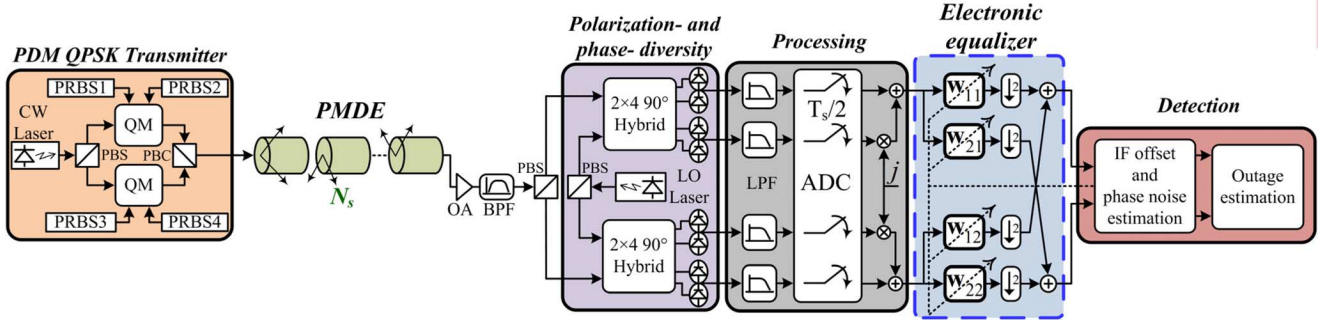


Fig. 1. System block diagram (Abbreviations: CW: continuous wave, PRBS: pseudorandom bit sequence, QM: quadrature modulator, PBS: polarization beam splitter, PBC: polarization beam combiner, PMDE: PMD emulator, N_s : number of sections, OA: optical amplifier, BPF: bandpass filter, LO: local oscillator, LPF: lowpass filter, T_s : symbol period, w : FIR filter taps, IF: intermediate frequency, Symbol \downarrow^2 : downsampling to one sample/symbol).

period) can reduce the outage probability to less than 10^{-5} , for a mean differential group delay (DGD) equal to one symbol period. However, CMA equalizers perform slightly better than the DD-LMS equalizers at links with larger DGD values, whereas the opposite holds true at the weak PMD regime. This is the reason behind the enhanced performance obtained when DD-LMS equalization is used after a first round of CMA-based equalization, compared to the case where either algorithm is used alone [4]. For instance, for strong PMD, e.g., when the mean DGD is equal to twice the symbol period, the successive application of CMA- and LMS-based equalization is beneficial because the former reduces the PMD enough so that the latter can perform more efficiently. This way, the transmission distance can be significantly improved.

It is worth noting that the presence of even a small intermediate frequency (IF) offset significantly affects the performance of the DD-LMS in the weak PMD regime. This indicates that CMA and its variants are most suitable adaptation algorithms for practical coherent PDM QPSK systems, where IF offset is nonnegligible.

The rest of the paper is organized as follows. In Section II, the simulation model of a coherent PDM QPSK system and the MMC method are presented. In Section III, we focus on quantifying the performance of the aforementioned linear adaptive electronic equalizers with respect to the outage probability of coherent PDM QPSK systems. This comparison is performed for a different number of equalizer coefficients and various system margins with and without IF offset. Some concluding remarks are given in Section IV.

II. THEORETICAL MODEL

A. Simulation Setup

The block diagram of the coherent PDM QPSK system under study is shown in Fig. 1. At the transmitter, two inde-

pendently modulated orthogonal polarization tributaries with nonreturn-to-zero QPSK pulses are generated. The symbol rate is denoted by $R_s = T_s^{-1}$. In our simulations, pseudorandom quaternary de Bruijn symbol sequences of length 4^{2d+1} are used, in order to take into account the intersymbol interference caused by all possible combinations of $2d + 1$ symbols.

The PMDE used in our simulations is comprised of a concatenation of N_s birefringent waveplates. Each birefringent waveplate is characterized by three random variables, namely $\{\alpha_m, \varepsilon_m, \Delta\tau_m\}$, where $\{\alpha_m, \varepsilon_m\}$ are the azimuth and ellipticity of the slow principal axis and $\{\Delta\tau_m\}$ is the DGD.

The transfer matrix \mathbf{M}_m of each birefringent waveplate is the product of two terms: 1) a 2×2 unitary Jones matrix \mathbf{R}_m , representing a rotation of the input state of polarization by a polarization controller [39]; and 2) a diagonal 2×2 Jones matrix \mathbf{D}_m [40], representing the birefringence of each fiber section [40]. Each transfer matrix \mathbf{M}_m is written as

$$\mathbf{M}_m = \mathbf{D}(\omega, \Delta\tau_m)\mathbf{R}(\alpha_m, \varepsilon_m), \quad m = 1, \dots, N_s \quad (1)$$

where ω is the angular frequency deviation from the signal optical carrier frequency. In (1), the matrices \mathbf{D} and \mathbf{R} are expressed as (2) and (3) shown at the bottom of the page [39].

In this paper, we exclusively focus on PMD. Therefore, PDL, chromatic dispersion, fiber nonlinearities, and laser's phase noise are neglected, in order to keep the simulation model as computationally efficient as possible.

On the receiver side, a coherent, homodyne, polarization- and phase-diversity optical front end is used, consisting of ideal 2×4 90° optical hybrids and balanced detectors, followed by fourth-order Bessel low-pass filters with $0.8 R_s$ 3-dB bandwidth. The photocurrents are filtered and sampled at twice the symbol rate.

PMD compensation and polarization demultiplexing are performed using three types of adaptive MIMO electronic

$$\mathbf{D}(\omega, \Delta\tau) = \begin{bmatrix} e^{-\frac{i\omega\Delta\tau}{2}} & 0 \\ 0 & e^{\frac{i\omega\Delta\tau}{2}} \end{bmatrix} \quad (2)$$

$$\mathbf{R}(\alpha, \varepsilon) = \begin{bmatrix} \cos \alpha \cos \varepsilon - i \sin \alpha \sin \varepsilon & -\sin \alpha \cos \varepsilon + i \cos \alpha \sin \varepsilon \\ \sin \alpha \cos \varepsilon + i \cos \alpha \sin \varepsilon & \cos \alpha \cos \varepsilon + i \sin \alpha \sin \varepsilon \end{bmatrix}. \quad (3)$$

equalizers [4]. They are all composed of four parallel FIR filters of various lengths, connected in a butterfly structure, whose impulse responses are denoted in Fig. 1 by $w_{ij}, i, j = 2$. We focus on fractionally spaced equalizers because they exhibit better performance than their symbol-spaced counterparts, due to their increased bandwidth and their timing-offset tolerance [41]. The DD-LMS algorithm [1], [25] is often used for the adaptive update of the equalizer's coefficients, due to its simplicity, good performance, and fast convergence. It is accompanied by a symbol-by-symbol phase tracking module [25]. A common alternative to the DD-LMS adaptation algorithm is the CMA. It is widely used for combined blind adaptive feed-forward polarization demultiplexing [5], [6] and PMD/PDL equalization [1], [4], [6], [21], [29]. The popularity of these CMA-based modules is due to their low computational complexity and their robustness in the presence of IF offsets and laser phase noise. The second feature allows for decoupling between polarization demultiplexing and carrier frequency/phase recovery, so the latter two impairments can be addressed by separate DSP modules [5]. Feed-forward frequency and phase-error estimators are used [5] to remove any small residual constellation rotations.

The PMD-induced OSNR penalty is used to determine whether an outage occurs or not. The OSNR penalty is defined as the difference in OSNR, expressed in decibels, between the back-to-back case and after transmission, required to achieve an error probability of 10^{-9} . The error probability is estimated using a semianalytical method [42]. The outage probability is defined as the probability that the OSNR penalty exceeds a specified threshold (system margin). We arbitrarily choose an outage probability of 10^{-5} as our design criterion [43], [44], which translates into a fractional outage time of 5.4 min per year.

B. MMC Method

The main idea of all importance sampling methods [16], [17], is to artificially generate events in the desired areas of the probability density function (pdf) of a random variable. Actually, in MMC simulations, the objective is to accurately evaluate the tails of the pdf of an unknown output random variable through an intentional biasing of the statistics of the input random variables. To optimize the number of samples falling in the target pdf tails, the generation of input samples is recursively biased.

For instance, assume that we want to evaluate the statistics of an output random variable Y , whose pdf is unknown. Assume that Y is linked through a function $Y = f(\mathbf{X})$ to an array \mathbf{X} of M input random variables X_1, \dots, X_M , whose joint pdf $p(\mathbf{X})$ is known. During the i th iteration of the MMC algorithm, a set of n input random arrays $\{\mathbf{X}_1, \dots, \mathbf{X}_n\}$ is generated, based on the Metropolis–Hastings algorithm [46]. The corresponding values of the output random variable $Y_1^{(i)}, \dots, Y_n^{(i)}$ are obtained and their histogram, over a prespecified number of bins, is constructed. At the end of i th iteration, the probability $\hat{P}_k^{(i)}$ of Y falling into the k th bin is calculated [30]. In subsequent iterations, the information of the estimated probability $\hat{P}_k^{(i)}$ is used to bias the input joint pdf $p^*(\mathbf{X})$, in order to produce further occurrences of Y on the tails of the desired output pdf $p(Y)$. Consequently, one obtains a more accurate estimation of the tails of the output pdf after a fairly small number of iterations.

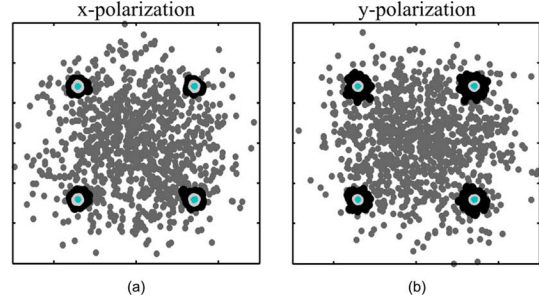


Fig. 2. Representative constellation diagrams of the two polarization tributaries, in the presence of PMD, before and after compensation. Symbols: uncompensated case (dark gray dots) and after a CMA equalizer with five taps (black dots), ten taps (light gray dots), and 15 taps (blue dots), for an instantaneous DGD equal to $2.8T_s$.

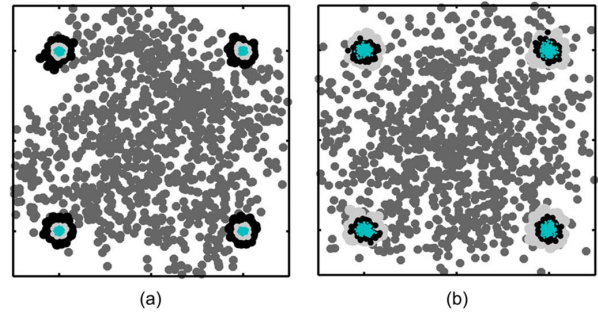


Fig. 3. Constellation diagrams of the x -polarization tributary for a normalized instantaneous DGD (a) of $0.64T_s$ (weak PMD regime) and (b) of $2.25T_s$ (strong PMD regime). Symbols: uncompensated case, i.e., one-tap, constrained CMA-based polarization demultiplexer (dark gray dots), equalizers with ten $T_s/2$ -spaced taps: DD-LMS (light gray dots); CMA (black dots); CMA/LMS (blue dots).

For the problem under study, the PMDE is modeled as a concatenation of $N_s = 30$ birefringent sections. In [45] and [46], it was shown that the instantaneous DGD of a PMDE composed of, at least, 15 birefringent sections follows a Maxwellian pdf with sufficient accuracy, if the DGD of each section is controlled to follow a Gaussian distribution and the principal states of polarization are uniformly distributed on the Poincaré sphere [45], [46]. During each of the ten MMC iterations, $n = 1000$ fiber realizations of the PMDE are generated and the histogram of the OSNR penalty's target pdf is constructed with 100 bins. In each MMC case study, the input random variables are the PMD parameters of each birefringent fiber section, i.e., the triplets $\{\alpha_m, \varepsilon_m, \Delta\tau_m\}$ mentioned in Section II-A. At each step of the Markov chain [47], candidate samples of the angular variables $\{\vec{\vartheta}_m\} = \{\alpha_m, \varepsilon_m\}$ are generated using the recursion $\{\vec{\vartheta}_m^*\} = \{\vec{\vartheta}_{m-1}\} + \{\delta\vec{\vartheta}_m\}$ where $\{\vec{\vartheta}_{m-1}\}$ are the current samples and $\{\delta\vec{\vartheta}_m\}$ are random increments following a uniform pdf $\{\delta\vec{\vartheta}_m\} \sim \xi_{\{\alpha, \varepsilon\}} \cdot U(-A, A)$, where $U(-A, A)$ denotes the uniform distribution in the range $[-A, A]$. The perturbation coefficient $\xi_{\{\alpha, \varepsilon\}}$ has a different value for each one of the angular variables $\{\alpha_m, \varepsilon_m\}$. The perturbation coefficients $\xi_{\{\alpha, \varepsilon\}}$ are set by trial and error. A useful criterion for their selection is the acceptance ratio, defined as the fraction of the accepted candidate Metropolis steps to the total number of Metropolis steps. As a rule of thumb, $\xi_{\{\alpha, \varepsilon\}}$ were selected in such a way that the acceptance ratio is about 20–50% [16], [17], [35]. For

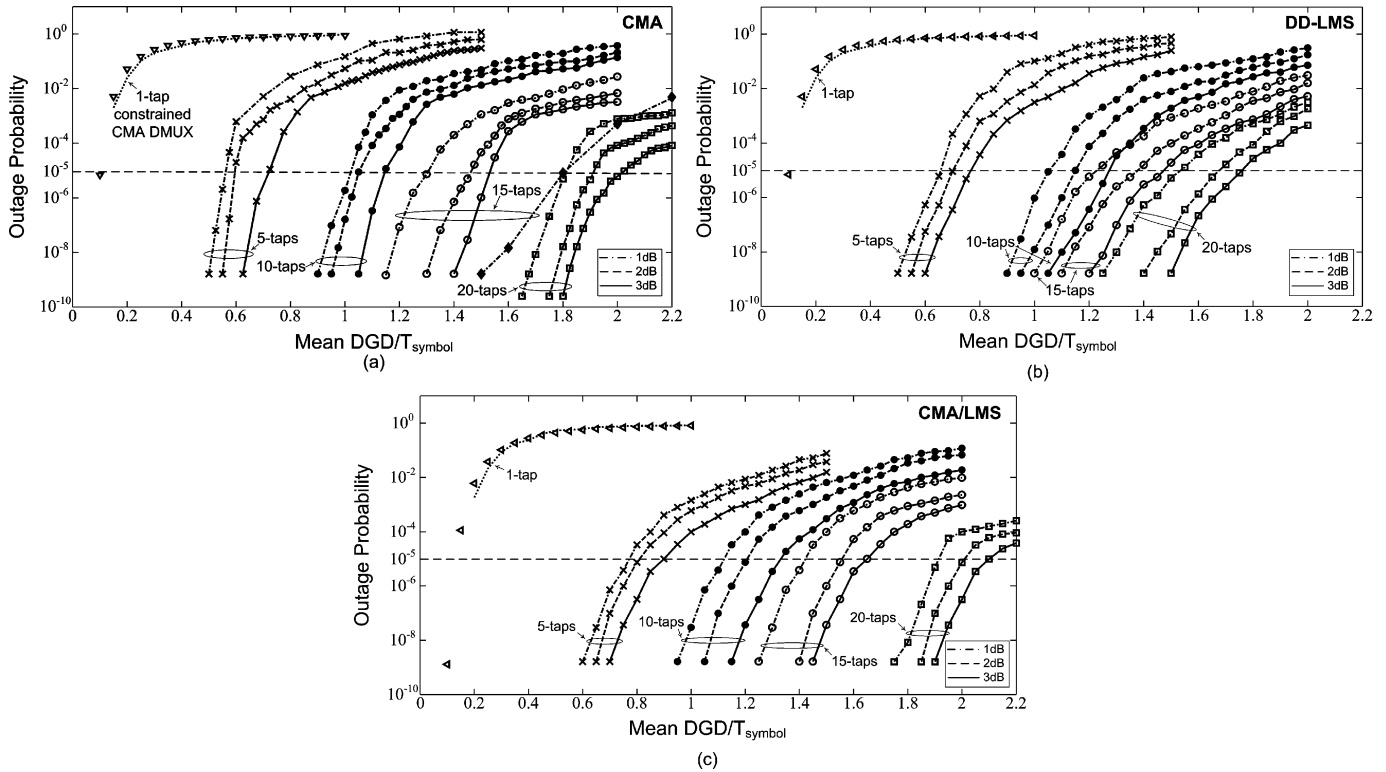


Fig. 4. Outage probability as a function of the normalized mean DGD. (a) CMA-based equalizer. (b) DD-LMS-based equalizer. (c) CMA/LMS-based equalizer. In (a), the dash-dotted line with the diamonds represents the case when a first-order PMDE and a 15-tap CMA equalizer are used. (Symbols: dotted line: one-tap polarization demultiplexer; triangles: analytical prediction using Antonelli's model [48] modified for uncompensated coherent PDM QPSK systems; crosses: five taps; filled circles: ten taps; open circles: 15 taps; diamonds: 15 taps and first-order PMDE; squares: 20 taps; dash-dotted line: 1-dB margin; dashed line: 2-dB margin; solid line: 3-dB margin).

the azimuth, the constant A is equal to $\pi/2$ and for the ellipticity is equal to $\pi/4$, respectively. The statistics of α_m , ε_m lead the corresponding PMD vectors to be uniformly distributed over the Poincaré sphere [45], [46], [48]. The DGDs $\Delta\tau_m$ of the individual fiber sections are assumed independent, identically distributed Gaussian random variables and the creation of a small perturbation is based on the Gaussian pdf $\delta\Delta\tau_m \sim \xi_{\Delta\tau} N(\mu, \sigma)$, where $N(\mu, \sigma)$ denotes the normal distribution with mean value $\mu = \sqrt{3\pi/8N_s} \langle \Delta\tau \rangle$ and standard deviation $\sigma = 0.2 \cdot \mu$, where $\langle \Delta\tau \rangle$ is the mean total DGD of the PMD emulation model, with angled brackets denoting ensemble average [7]. These assumptions lead to a Maxwellian pdf for the total instantaneous DGD [45], [46], [48].

The structure of the MMC algorithm lends itself to parallel implementation [37]. Parallelization, here, is performed at two levels: 1) different runs corresponding to different mean total DGD values are launched on different computers (embarrassingly parallel application); 2) within a single run, concurrent execution of commands within “for loops” is achieved by using different cores on a multicore computer. The purpose is to perform multiple simulation runs of the same model for different input settings. The execution environment is an interactive parallel one in which the parallel implemented code is executed. In this environment, parallel for loops and distributed arrays automatically detect the presence of cores and distribute computations between the cores. Using concurrent loop execution, we managed to accelerate the execution time for each separate MMC simulation up to three times by using four cores of a Quad Intel processor.

III. RESULTS AND DISCUSSION

A qualitative comparison of the performance of adaptive electronic CMA-based equalizers with respect to the uncompensated case, with various numbers of taps, is shown in Fig. 2. Here, the term “uncompensated” means a coherent optical system with a one symbol-spaced tap, constrained CMA electronic demultiplexer [5]. Fig. 2 shows representative constellation diagrams obtained during the last MMC iteration for the uncompensated case (dark gray dots), as well as for CMA-based equalizers using FIR filters with five taps (black dots), ten taps (light gray dots), and 15 taps (blue dots) each. In this particular case, the instantaneous DGD is equal to $2.8T_s$. As expected, when the number of FIR filter taps increases, the constellation diagrams of both polarization tributaries are gradually improved.

A qualitative performance comparison among ten-tap $T_s/2$ -spaced CMA-based equalizers, DD-LMS-based equalizers, and their combination is shown in Fig. 3(a) and (b) for two values of instantaneous DGD. Constellation diagrams for the uncompensated case (dark gray points) and after the aforementioned equalizers (various colors) are shown. These results illustrate our claim that CMA equalizers (black dots) perform better than their DD-LMS counterparts (light gray dots) in the strong PMD regime, contrary to the weak PMD regime, where DD-LMS equalizers are superior. We observe that the successive application of CMA- and DD-LMS-based equalization (blue dots) always offers better performance compared to either stand-alone equalizers, under the same PMD conditions.

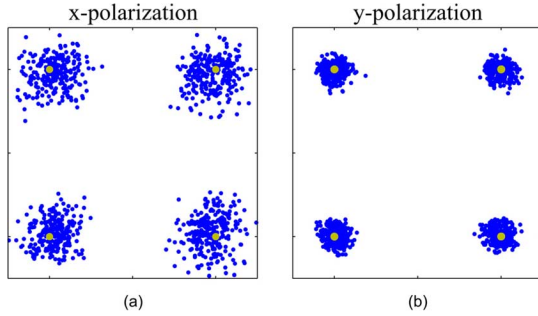


Fig. 5. Constellation diagrams of the two polarization tributaries after equalization using an all-order (blue dots) and a first-order PMDE (yellow dots) with the same instantaneous first-order PMD vector. Conditions: 15-tap CMA equalizer for an instantaneous DGD of $2.2T_s$.

Subsequently, the outage probability after equalization is evaluated, as a function of the normalized mean DGD, for various system margins, in the absence of IF offset. Numerical results are shown in Fig. 4(a) for CMA-based equalizers, in Fig. 4(b) for DD-LMS-based equalizers, and in Fig. 4(c) for their combination. We observe that all aforementioned equalizer types significantly reduce the impact of PMD. For instance, the CMA equalizer considerably increases the maximum tolerable mean DGD to $0.58T_s$, when five taps per FIR filter are used, and to $1.8T_s$, when 20 taps per FIR filter are used, assuming a 1-dB system margin, at an outage probability of 10^{-5} . Furthermore, in Fig. 4(a), we observe that, if we change the system margin from 1 to 3 dB, the acceptable mean DGD increases by about 25%, independent of the number of taps, assuming an outage probability of 10^{-5} . For instance, the 20-tap CMA equalizer can increase the tolerable mean DGD values to $2.05T_s$, for a 3-dB threshold.

It is worth noting that the performance evaluation of various equalizers using first-order PMDEs [1] is optimistic. The reason for this is that higher order PMD significantly affects equalizer performance.

Figs. 4(a) and 5 illustrate the earlier claim. According to Fig. 4(a), if only first-order PMD is emulated, a CMA equalizer with 15 taps per FIR filter can tolerate a mean DGD up to $1.8T_s$ [see dash-dotted curve with diamonds in Fig. 4(a)]. In contrast, the same equalizer can tolerate a mean DGD of only $1.3T_s$, when higher order PMD is also taken into account. A qualitative explanation for this discrepancy is provided by Fig. 5. In Fig. 5, we show indicative constellation diagrams after PMD equalization using a 15-tap CMA-based equalizer, for an instantaneous DGD equal to $1.5T_s$ at an outage probability of 10^{-5} , for 1-dB margin. Yellow points are obtained using a first-order PMDE and blue points using an all-order PMDE with the same first-order PMD vector as the initial one. It is quite obvious that results obtained using a first-order PMDE can be misleading [1], [28].

Returning back to Fig. 4, it is worth noting that CMA-based equalizers are more robust than their DD-LMS counterparts, in the strong PMD regime. For instance, as mentioned earlier, CMA-based equalizers with $20T_s/2$ -spaced taps per FIR filter can compensate for a mean DGD equal to $1.8T_s$ at an outage probability of 10^{-5} and for a 1-dB system margin [see Fig. 4(a)]. In contrast, similar DD-LMS equalizers can

compensate only for a mean DGD of $1.52T_s$ under the same conditions [Fig. 4(b)]. Therefore, the use of CMA-based equalizers leads to an 18.4% increase of the acceptable mean DGD or, equivalently, to a 40.2% longer transmission distance. These results change slightly if the PMD margin is relaxed from 1 to 3 dB in Fig. 4(a) and (b). We observe that the acceptable mean DGD increases significantly for both equalizer types but not by the same amount. For instance, it is possible to achieve a 36.7% longer transmission distance for a 15-tap CMA-based equalizer (increasing mean tolerable DGD from $1.32T_s$ at 1 dB to $1.55T_s$ at 3 dB) compared to 47.2% for a 15-tap DD-LMS-based equalizer (increasing mean tolerable DGD from $1.24T_s$ at 1 dB to $1.47T_s$ at 3 dB) under the same conditions. Nevertheless, the aforementioned trend in favor of CMA still holds.

The comparison of the performance of stand-alone CMA-based [see Fig. 4(a)] and DD-LMS-based [see Fig. 4(b)] equalizers against their combination [see Fig. 4(c)], with $20T_s/2$ -spaced taps per FIR filter, shows that the latter can tolerate a 6.67% larger mean total DGD, at an outage probability of 10^{-5} , for 1-dB margin, for zero IF offset. The superior performance of the CMA/LMS equalizer holds for both the weak and the strong PMD regime. The tolerable mean DGD is allowed to increase up to $1.58T_s$, using only 15 taps, for a 2-dB system margin and for an outage probability of 10^{-5} .

In the weak PMD regime, the performance of DD-LMS-based equalizer is superior. For instance, the CMA-based equalizer with five taps can compensate for a mean DGD of $0.58T_s$ [see Fig. 4(a)], as opposed to $0.65T_s$ for their LMS-based counterparts, at an outage probability of 10^{-5} and a 1-dB system margin [see Fig. 4(b)]. We caution the reader that the previous conclusions hold for zero IF offset.

Finally, we performed a sanity check for the accuracy of the results of MMC by comparing them to the results of the approximate analytical model of [49], modified for uncompensated coherent PDM QPSK systems (using a constrained CMA-based polarization demultiplexer with a one tap per filter). The theoretical prediction (triangles) is fairly close to simulation results (dotted line), as shown in Fig. 4. We also verified, by conventional MC simulations, the validity of the results of MMC simulations corresponding to high outage probabilities in Fig. 4(a)–(c).

Figs. 6 and 7 show that the existence of IF offset degrades the performance of the DD-LMS-based equalizer, indicating that the CMA-based equalizer is a more suitable candidate for use in a practical coherent PDM QPSK system, even in the weak PMD regime.

More specifically, in Fig. 6, we investigate the performance of five-tap CMA-based and DD-LMS equalizers in the presence of an IF offset equal to $0.02R_s$ in a coherent PDM QPSK system. For the five-tap CMA-based equalizer, at an outage probability of 10^{-5} , the tolerable mean DGD value is decreased by 15% for a 1-dB OSNR margin, whereas for a 2- and a 3-dB margin it is decreased by 3.3% and 4.2%, respectively. On the contrary, for the five-tap DD-LMS-based equalizer, at an outage probability of 10^{-5} , the tolerable mean DGD value is decreased by 35% for a 1-dB OSNR margin, whereas for a 2- and a 3-dB margin it is decreased by 25% and 18.2%, respectively.

Fig. 7 shows that, for the ten-tap CMA-based equalizer and at an outage probability of 10^{-5} , the tolerable mean DGD value

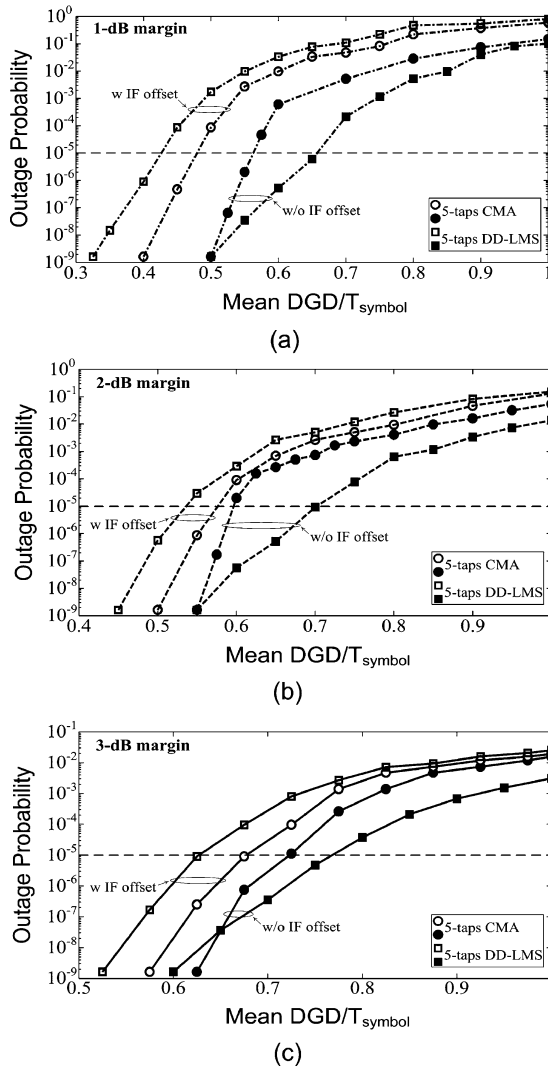


Fig. 6. Outage probability as a function of the normalized mean DGD. (a) 1-dB margin. (b) 2-dB margin. (c) 3-dB margin. (Symbols: open circles: five-tap CMA-based equalizer in the presence of IF offset; filled circles: five-tap CMA-based equalizer in the absence of IF offset; open squares: five-tap DD-LMS-based equalizer in the presence of IF offset; filled squares: five-tap DD-LMS-based equalizer in the absence of IF offset).

is decreased by only 6.8% for a 1-dB OSNR margin, whereas for a 2- and a 3-dB margin it is decreased by 5.6% and 1.8%, respectively. Under the same conditions, the performance of the DD-LMS-based equalizer declines more rapidly. For instance, the acceptable mean DGD values for a 1-dB OSNR margin decreases by 17.7%, whereas for a 2- and a 3-dB margin, it decreases by 16.5% and 14.8%, respectively.

IV. CONCLUSION

In this paper, we compared the performance of fractionally spaced, CMA-, DD-LMS- and CMA/LMS-based PMD equalizers in coherent PDM QPSK systems in the exclusive presence of PMD. The outage probability was used as a performance criterion. Very rare PMD events were generated using a parallel programming implementation of the MMC method. In the absence of IF offset, it was shown that CMA equalizers perform

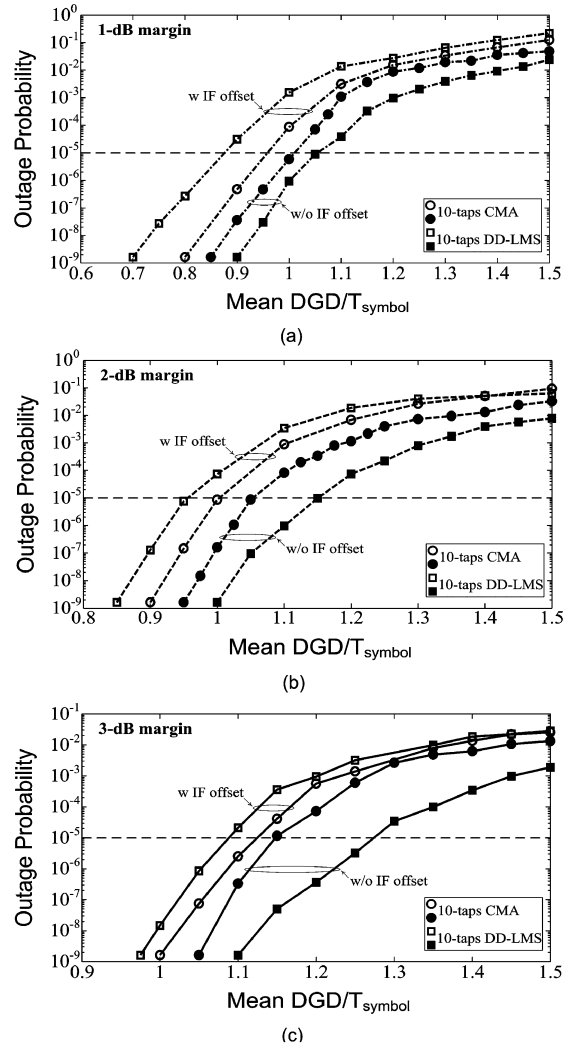


Fig. 7. Outage probability as a function of the normalized mean DGD. (a) 1-dB margin. (b) 2-dB margin. (c) 3-dB margin. (Symbols: open circles: ten-tap CMA-based equalizer in the presence of IF offset; filled circles: ten-tap CMA-based equalizer in the absence of IF offset; open squares: ten-tap DD-LMS-based equalizer in the presence of IF offset; filled squares: ten-tap DD-LMS-based equalizer in the absence of IF offset).

slightly better than their DD-LMS counterparts in the strong PMD regime, whereas the opposite holds true at the weak PMD regime. In the presence of IF offset, the CMA-based equalizer is a more suitable candidate for practical coherent PDM QPSK systems. In all cases, successive application of these adaptive equalization algorithms offers a better performance than either one alone.

ACKNOWLEDGMENT

The authors would like to thank Prof. A. Bononi, Prof. P. Serena, and Mr. N. Rossi, University of Parma, as well as Mr. A. Ghazisaeidi, Université Laval, Canada, for their help in the understanding of the MMC method. They would also like to thank Prof. N. Antoniadis, Mr. P. Muzio, and Mr. C. Lee, CUNY, College of Staten Island, for their help in testing early versions of the parallel MMC program at the CUNY high-performance computing facility.

REFERENCES

- [1] C. R. S. Fludger, T. Duthel, D. van den Borne, C. Schullien, E. D. Schmidt, T. Wuth, J. Geyer, E. De Man, G. D. Khoe, and H. de Waardt, "Coherent equalization and POLMUX-RZ-DQPSK for robust 100-GE transmission," *J. Lightw. Technol.*, vol. 26, no. 1, pp. 64–72, Jan. 2008.
- [2] J. Renaudier, G. Charlet, M. Salsi, O. B. Pardo, H. Mardoyan, P. Tran, and S. Bigo, "Linear fiber impairments mitigation of 40-Gbit/s polarization-multiplexed QPSK by digital processing in a coherent receiver," *J. Lightw. Technol.*, vol. 26, no. 1, pp. 36–42, Jan. 2008.
- [3] L. E. Nelson, S. L. Woodward, S. Foo, X. Zhou, M. D. Feuer, D. Hanson, D. McGhan, H. Sun, M. Moyer, M. O. Sullivan, and P. D. Magill, "Performance of a 46-Gbps dual-polarization QPSK transceiver with real-time coherent equalization over high PMD fiber," *J. Lightw. Technol.*, vol. 27, no. 3, pp. 158–167, Feb. 2009.
- [4] S. J. Savory, "Digital filters for coherent optical receivers," *Opt. Exp.*, vol. 16, no. 2, pp. 804–817, Jan. 2008.
- [5] I. Roudas, A. Vgenis, C. S. Petrou, D. Toumpakaris, J. Hurley, M. Sauer, J. Downie, Y. Mauro, and S. Raghavan, "Optimal polarization demultiplexing for coherent optical communications systems," *J. Lightw. Technol.*, vol. 28, no. 7, pp. 1121–1134, Apr. 2010.
- [6] A. Vgenis, C. S. Petrou, C. B. Papadias, I. Roudas, and L. Raptis, "Non-singular constant modulus equalizer for PDM-QPSK coherent optical receivers," *IEEE Photon. Technol. Lett.*, vol. 22, no. 1, pp. 45–47, Jan. 2010.
- [7] H. Sunnerud, M. Karlsson, C. Xie, and P. A. Andrekson, "Polarization-mode dispersion in high-speed fiber-optic transmission systems," *J. Lightw. Technol.*, vol. 20, no. 12, pp. 2204–2219, Dec. 2002.
- [8] C. Xie, L. Möller, H. Haunstein, and S. Hunsche, "Comparison of system tolerance to polarization-mode dispersion between different modulation formats," *IEEE Photon. Technol. Lett.*, vol. 15, no. 8, pp. 1168–1170, Aug. 2003.
- [9] P. J. Winzer, H. Kogelnik, C. H. Kim, R. M. Jopson, L. E. Nelson, and K. Ramanan, "Receiver impact on first order PMD outage," *IEEE Photon. Technol. Lett.*, vol. 15, no. 10, pp. 1482–1484, Oct. 2003.
- [10] P. J. Winzer, H. Kogelnik, and K. Ramanan, "Precise outage specifications for first-order PMD," *IEEE Photon. Technol. Lett.*, vol. 16, no. 2, pp. 449–451, Feb. 2004.
- [11] H. Kogelnik, L. E. Nelson, and P. J. Winzer, "Second-order PMD outage of first-order compensated fiber systems," *IEEE Photon. Technol. Lett.*, vol. 16, no. 4, pp. 1053–1055, Apr. 2004.
- [12] E. Forestieri and G. Prati, "Exact analytical evaluation of second-order PMD impact on the outage probability for a compensated system," *J. Lightw. Technol.*, vol. 22, no. 4, pp. 988–996, Apr. 2004.
- [13] F. Buchali and H. Bülow, "Adaptive PMD compensation by electrical and optical techniques," *J. Lightw. Technol.*, vol. 22, no. 4, pp. 1116–1126, Apr. 2004.
- [14] H. Bülow, F. Buchali, and A. Klekamp, "Electronic dispersion compensation," *J. Lightw. Technol.*, vol. 26, no. 1, pp. 158–167, Jan. 2008.
- [15] C. Xie, X. Liu, and H. Bülow, "PMD-induced outage probability in an optical communication system with fast polarization scramblers and time-varying PMD sections," *IEEE Photon. Technol. Lett.*, vol. 20, no. 6, pp. 440–442, Mar. 2008.
- [16] G. Biondini, W. L. Kath, and C. R. Menyuk, "Importance sampling for polarization-mode dispersion: Techniques and applications," *J. Lightw. Technol.*, vol. 22, no. 4, pp. 1201–1215, Apr. 2004.
- [17] A. O. Lima, C. R. Menyuk, and I. T. Lima, "Comparison of two biasing Monte Carlo methods for calculating outage probabilities in systems with multisection PMD compensators," *IEEE Photon. Technol. Lett.*, vol. 17, no. 12, pp. 2580–2582, Dec. 2005.
- [18] P. Lu, L. Chen, and X. Bao, "System outage probability due to the combined effect of PMD and PDL," *J. Lightw. Technol.*, vol. 21, no. 10, pp. 1805–1808, Oct. 2002.
- [19] B. L. Heffner, "Simplified calculation of system outage caused by polarization-mode dispersion," *IEEE Photon. Technol. Lett.*, vol. 20, no. 12, pp. 1069–1071, Jun. 2008.
- [20] M. Boroditsky, M. Brodsky, N. J. Frigo, P. Magill, C. Antonelli, and A. Mecozzi, "Outage probabilities for fiber routes with finite number of degrees of freedom," *IEEE Photon. Technol. Lett.*, vol. 17, no. 2, pp. 345–347, Feb. 2005.
- [21] S. J. Savory, F. Payne, and A. Hadjifotiou, "Estimating outages due to polarization mode dispersion using extreme value statistics," *J. Lightw. Technol.*, vol. 24, no. 11, pp. 3907–3913, Nov. 2006.
- [22] M. H. Smith and R. A. Chipman, "Comparison of different PMD compensator configurations based on outage probability," in *Proc. Opt. Fiber Commun. Conf.*, San Jose, CA, 2002, pp. 233–234.
- [23] E. Ip and J. M. Kahn, "Digital equalization of chromatic dispersion and polarization mode dispersion," *J. Lightw. Technol.*, vol. 25, no. 8, pp. 2033–2043, Aug. 2007.
- [24] M. Kuschnerov, F. N. Hauske, K. Piyawanno, B. Spinnler, M. S. Alfiad, A. Napoli, and B. Lankl, "DSP for coherent single-carrier receivers," *J. Lightw. Technol.*, vol. 27, no. 16, pp. 3614–3622, Aug. 2009.
- [25] D. E. Crivelli, H. S. Carrer, and M. R. Hueda, "Adaptive digital equalization in the presence of chromatic dispersion, PMD, and phase noise in coherent fiber optic systems," in *Proc. IEEE Commun. Soc. Globecom*, 2004, pp. 2545–2551.
- [26] M. S. Alfiad, D. van den Borne, S. L. Jansen, T. Wuth, M. Kuschnerov, G. Grosso, A. Napoli, and H. de Waardt, "A comparison of electrical and optical dispersion compensation for 111-Gb/s POLMUX RZ-DQPSK," *J. Lightw. Technol.*, vol. 27, no. 16, pp. 3590–3598, Aug. 2009.
- [27] A. T. Erdogan, A. Demir, and T. M. Oktem, "Automatic PMD compensation by unsupervised polarization diversity combining coherent receivers," *J. Lightw. Technol.*, vol. 26, no. 13, pp. 1823–1834, Jul. 2008.
- [28] C. Remmersmann, M. Westhäuser, S. Pachnicke, G. Göger, G. Kerner, and P. M. Krümmrich, "Equalization of first and second order PMD in 100 Gbit/s PolMux transmission using optical butterfly FIR filters," presented at the presented at the Opt. Fiber Commun. Conf., San Diego, CA, 2010, OThj3.
- [29] C. Xie and S. Chandrasekhar, "Two-Stage CMA equalizer for singularity free operation and optical performance monitoring in optical coherent receiver," presented at the presented at the Opt. Fiber Commun. Conf., San Diego, CA, 2010, OMK3.
- [30] D. Yevick, "Multicanonical communication system modelling-application to PMD statistics," *IEEE Photon. Technol. Lett.*, vol. 14, no. 11, pp. 1512–1514, Nov. 2002.
- [31] D. Yevick, "The accuracy of multicanonical system models," *IEEE Photon. Technol. Lett.*, vol. 15, no. 2, pp. 224–226, Feb. 2003.
- [32] T. Lu and D. Yevick, "Efficient multicanonical algorithms," *IEEE Photon. Technol. Lett.*, vol. 17, no. 4, pp. 861–863, Apr. 2005.
- [33] T. Kamalakis, D. Varoutas, and T. Spicopoulos, "Statistical study of in band crosstalk noise using the multicanonical Monte Carlo method," *IEEE Photon. Technol. Lett.*, vol. 16, no. 10, pp. 2242–2244, Oct. 2004.
- [34] A. Bilenca, A. Desjardins, B. E. Bouma, and G. J. Tearney, "Multicanonical Monte Carlo simulations of light propagation in biological media," *Opt. Exp.*, vol. 13, no. 24, pp. 9822–9833, Nov. 2005.
- [35] A. Bononi, "Multicanonical Monte Carlo and importance sampling simulation techniques: How are they related?," in Notes of a Course For Ph.D. Students in Information Engineering Italy, Jan. 2007, Univ. Parma.
- [36] A. Bononi, L. A. Rusch, A. Ghazisaeidi, F. Vacondio, and N. Rossi, "A fresh look at multicanonical Monte Carlo from a telecom perspective," in *Proc. IEEE Commun. Soc. Globecom*, Honolulu, HI, 2009, pp. 1–8, CTS-14.
- [37] A. Ghazisaeidi, F. Vacondio, and L. A. Rusch, "Filter design for SOA-assisted SS-WDM systems using parallel multicanonical Monte Carlo," *J. Lightw. Technol.*, vol. 28, no. 1, pp. 79–90, Jan. 2010.
- [38] S. Haykin, *Adaptive Filter Theory*, 3rd ed. Englewood Cliffs, NJ: Prentice-Hall, 1996.
- [39] D. Penninckx and V. Morénas, "Jones matrix of polarization mode dispersion," *Opt. Lett.*, vol. 24, no. 13, pp. 875–877, Jul. 1999.
- [40] J. P. Gordon and H. Kogelnik, "PMD fundamentals: Polarization mode dispersion in optical fibers," in *Proc. Nat. Acad. Sci.*, 2000, vol. 97, pp. 4541–4550.
- [41] S. H. U. Qureshi and G. D. Forney, "Performance and properties of a T/2 equalizer," in *Nat. Telecommun. Conf.*, 1977, pp. 11.1.1–11.1.9.
- [42] M. C. Jeruchim, P. Balaban, and K. S. Shanmugan, *Simulation of Communication Systems: Modeling, Methodology and Techniques*. Berlin, Germany: Springer-Verlag, 2000.
- [43] H. Kogelnik, R. M. Jopson, and L. E. Nelson, I. P. Kaminow and T. L. Koch, Eds., "Polarization-mode dispersion," in *Optical Fiber Telecommunications*. San Diego, CA: Academic, 1997, vol. IVB, ch. 15.
- [44] J. Poirrier, M. Gadonna, and L. Dupont, "PMD effects in fiber optic transmission systems," *Fiber Integr. Opt.*, vol. 27, pp. 559–578, Nov. 2008.
- [45] R. Khosravani, I. T. Lima, Jr., P. Ebrahimi, E. Ibragimov, A. E. Willner, and C. R. Menyuk, "Time and frequency domain characteristics of polarization-mode dispersion emulators," *IEEE Photon. Technol. Lett.*, vol. 13, no. 2, pp. 127–129, Feb. 2001.
- [46] J. H. Lee, M. S. Kim, and Y. C. Chung, "Statistical PMD emulator using variable DGD elements," *IEEE Photon. Technol. Lett.*, vol. 15, no. 1, pp. 54–56, Jan. 2003.

- [47] N. Metropolis, A. W. Rosenbluth, M. N. Rosenbluth, A. H. Teller, and E. Teller, "Equations of state calculations by fast computing machines," *J. Chem. Phys.*, vol. 21, no. 6, pp. 1087–1092, Jun. 1953.
- [48] N. Mantzoukis, C. S. Petrou, A. Vgenis, I. Roudas, T. Kamalakis, and L. Raptis, "Electronic equalization of polarization mode dispersion in coherent POL-MUX QPSK systems," presented at the presented at the Eur. Conf. Opt. Commun., Vienna, Austria, 2009, Paper P4.15.
- [49] C. Antonelli, A. Mecozzi, K. Cornick, M. Brodsky, and M. Boroditsky, "PMD-induced penalty statistics in fiber links," *IEEE Photon. Technol. Lett.*, vol. 17, no. 5, pp. 1013–1015, May 2005.

Nikolaos Mantzoukis was born in Corfu, Greece, in 1980. He received the B.Eng./M.Eng. and Ph.D. degrees in electrical and computer engineering from the University of Patras, Rio, Greece, in 2004 and 2010, respectively.

In 2005, he was involved in research programs in the field of emulation and equalization of the polarization-mode dispersion for coherent optical fiber communications with advanced modulation formats. His research interests include linear polarization-mode dispersion, multicanonical Monte Carlo method, and DSP algorithms for receivers.

Dr. Mantzoukis has been a member of the Technical Chamber of Greece since 2005. Since August 2010, he has been serving his military service at the Hellenic Army Academy as a Network Administrator.

Constantinos S. Petrou (M'10) was born in Athens, Greece, in 1980. He received the B.Eng./M.Eng. and Ph.D. degrees in electrical and computer engineering from the University of Patras, Rio, Greece, in 2005 and 2010, respectively.

In 2005, he was involved in numerous research programs in the field of digital signal processing algorithms for coherent optical fiber communications with advanced modulation formats. In 2009, he joined Analogies S.A., where he is engaged in the research and development of forward error correction schemes for high-speed communications applications. He has served as a Researcher under contract with the European Space Agency in the field of low-density parity-check codes. He is the author and coauthor of two provisional patent applications, and large number of IEEE articles and international conference publications. His research interests include span forward error correction, modulation formats, and DSP algorithms for baseband receivers.

Dr. Petrou has been a member of the Technical Chamber of Greece since 2006, and has been a reviewer of IEEE PHOTONICS TECHNOLOGY LETTERS since 2009.

Athanasios Vgenis was born in Greece in 1981. He received both the diploma and Ph.D. degrees in electrical and computer engineering from the University of Patras, Rio, Greece, in 2005 and 2010, respectively.

He has taken part in several research projects, mostly, in the field of digital signal processing algorithms for electronic equalization in the area of coherent optical fiber communications, and has worked as an Electrical Engineer in the construction business. He is a member of T.o.m.Xw.k.as. His research interests include optical communications systems, optical coherent receivers, and electronic equalization of transmission effects.

Dr. Vgenis has been a member of the Technical Chamber of Greece since 2006.

Ioannis Roudas (M'00) received the B.S. degree in physics and the M.S. degree in electronics and radio engineering from the University of Athens, Athens, Greece, in 1988 and 1990, respectively, and the M.S. and Ph.D. degrees in coherent optical communication systems from the Ecole Nationale Supérieure des Télécommunications, Paris, France, in 1991 and 1995, respectively.

From 1995 to 1998, he was with the Optical Networking Research Department, Bell Communications Research (Bellcore), Red Bank, NJ. In addition, he was an Adjunct Professor of the graduate course entitled "Lightwave Systems" in the Electrical Engineering Department, Columbia University, New York, during the fall semesters of 1997 and 1998. From 1999 to 2002, he was with the Photonic Modeling and Process Engineering Department, Corning Incorporated, Somerset, NJ. He recently joined the Department of Electrical and Computer Engineering, University of Patras, Rio, Greece, as an Associate Professor of optical communications. He is the author or coauthor of more than 40 papers in scientific journals and international conferences and holds two patents.

Dr. Roudas serves as a Reviewer for the JOURNAL OF LIGHTWAVE TECHNOLOGY, the IEEE PHOTONICS TECHNOLOGY LETTERS, and *Optics Communications*.

Thomas Kamalakis was born in 1975. He received the B.Sc. degree in informatics and the M.Sc. degree (with distinction) in telecommunication from the University of Athens in 1997 and 1999, respectively. In 2004, he completed his Ph.D. thesis in the design and modeling of arrayed waveguide grating devices from the same institution.

Since 2008, he has been a Lecturer in the Department of Informatics and Telematics, Harokopio University of Athens. His research interests include photonic crystal and optical wireless devices as well as nonlinear effects in optical fibers.